Developmental Biology 462 (2020) 223–234

Contents lists available at ScienceDirect

Developmental Biology

journal homepage: www.elsevier.com/locate/developmentalbiology

Gon4l/Udu regulates cardiomyocyte proliferation and maintenance of ventricular chamber identity during zebrafish development

Terin E. Budine [a], Carmen de Sena-Tomás [b], Margot L.K. Williams [a], Diane S. Sepich [a], Kimara L. Targoff [b], Lila Solnica-Krezel [a,*]

[a] Department of Developmental Biology, Washington University School of Medicine, St. Louis, MO 63110, USA
[b] Division of Pediatric Cardiology, Department of Pediatrics, College of Physicians & Surgeons, Columbia University, 630 West 168th Street, New York, NY 10032, USA

ARTICLE INFO

Keywords:
Ugly duckling (*udu*)
nkx2.5
Heart development
Chamber identity
Proliferation

ABSTRACT

Vertebrate heart development requires spatiotemporal regulation of gene expression to specify cardiomyocytes, increase the cardiomyocyte population through proliferation, and to establish and maintain atrial and ventricular cardiac chamber identities. The evolutionarily conserved chromatin factor Gon4-like (Gon4l), encoded by the zebrafish *ugly duckling* (*udu*) locus, has previously been implicated in cell proliferation, cell survival, and specification of mesoderm-derived tissues including blood and somites, but its role in heart formation has not been studied. Here we report two distinct roles of Gon4l/Udu in heart development: regulation of cell proliferation and maintenance of ventricular identity. We show that zygotic loss of *udu* expression causes a significant reduction in cardiomyocyte number at one day post fertilization that becomes exacerbated during later development. We present evidence that the cardiomyocyte deficiency in *udu* mutants results from reduced cell proliferation, unlike hematopoietic deficiencies attributed to TP53-dependent apoptosis. We also demonstrate that expression of the G1/S-phase cell cycle regulator, *cyclin E2* (*ccne2*), is reduced in *udu* mutant hearts, and that the Gon4l protein associates with regulatory regions of the *ccne2* gene during early embryogenesis. Furthermore, *udu* mutant hearts exhibit a decrease in the proportion of ventricular cardiomyocytes compared to atrial cardiomyocytes, concomitant with progressive reduction of *nkx2.5* expression. We further demonstrate that *udu* and *nkx2.5* interact to maintain the proportion of ventricular cardiomyocytes during development. However, we find that ectopic expression of *nkx2.5* is not sufficient to restore ventricular chamber identity suggesting that Gon4l regulates cardiac chamber patterning via multiple pathways. Together, our findings define a novel role for zygotically-expressed Gon4l in coordinating cardiomyocyte proliferation and chamber identity maintenance during cardiac development.

1. Introduction

The heart is the first organ to form and function in the developing embryo (Bakkers, 2011). Defects in early heart development can result in congenital heart disease (CHD), which is the most common birth defect affecting nearly 1% of newborns (Pierpont et al., 2007; Triedman and Newburger, 2016). While much progress has been made in identifying the complex gene networks that specify, pattern, and shape the heart, the role of chromatin factors and how they regulate these networks are less well understood. Advancing knowledge of the gene regulatory cascade underlying normal heart development is essential for better diagnosis, treatment and prevention of CHDs.

Zebrafish embryos are an attractive model system in which to study cardiogenesis due to the rapidity of heart development and their ability to survive during embryogenesis without a functioning cardiovascular system (Bakkers, 2011). By 24 h post fertilization (hpf), a beating heart tube has formed and, over the next 24 h, it undergoes a series of gene expression and morphological changes that pattern and shape the atrial and ventricular chambers, respectively (Yelon, 1999). These two cardiac chambers expand in size through *de novo* differentiation of cardiac precursor cells (CPCs) and proliferation of existing cardiomyocytes (de Pater et al., 2009; Foglia and Poss, 2016). Several cardiac-specific transcription factors involved in cardiomyocyte specification and patterning of the cardiac chambers have been identified, among them T-box transcription factors, Nkx2.5, Gata4, Hey2, and Irx4 (Paige et al., 2015). Interestingly, loss-of-function mutations in these cardiac genes often lead to reduced

* Corresponding author.
E-mail address: solnical@wustl.edu (L. Solnica-Krezel).

https://doi.org/10.1016/j.ydbio.2020.03.002
Received 9 March 2018; Received in revised form 26 January 2020; Accepted 2 March 2020
Available online 6 April 2020

expression of ventricle-specific genes, suggesting that atrial fate might be a default state (Stainier, 2001; Yutzey, 1994, 1995).

Nkx2.5 is of particular interest among these transcriptional regulators as it plays critical roles throughout cardiac development, and these roles are evolutionarily conserved from fruit flies to humans (Bodmer, 1993; Harvey, 2002; Jay, 2003; Targoff et al., 2013). In zebrafish, *nkx2.5* and its paralog *nkx2.7* are expressed in the nascent cardiomyocytes during early development (Chen and Fishman, 1996; Lee et al., 1996; Reifers et al., 2000), and are later required for maintenance of ventricular identity (Targoff et al., 2008, 2013). Loss of *nkx2.5* expression results in reduced expression domains of ventricular genes, and inactivation of both *nkx2.5* and *nkx2.7* further enhances the deficiency of ventricular identity and leads to atrial cell-fate expansion (Targoff et al., 2013; Tu et al., 2009). Overexpression of *nkx2.5* compensates for loss of both *nkx2.5* and *nkx2.7,* indicating that these genes have largely redundant functions (George et al., 2015; Tu et al., 2009).

The nascent cardiomyocyte population expands through two distinct mechanisms: specification and proliferation of cardiomyocytes (de Pater et al., 2009; Foglia and Poss, 2016). During gastrulation, the first heart field is specified *de novo* in the anterior lateral plate mesoderm (ALPM) and, during segmentation, a cardiac cone is formed that elongates to become the linear heart tube (Buckingham et al., 2005; de Pater et al., 2009; Matrone et al., 2017; Rohr et al., 2006). Additional second heart field cardiomyocytes subsequently differentiate and contribute to the poles of the heart tube (de Pater et al., 2009). Cardiomyocytes proliferate during later segmentation stages and after heart tube formation to enlarge the developing heart (de Pater et al., 2009).

While much progress has been made in identifying the complex gene networks that specify cardiomyocytes, pattern and shape the heart, how these gene networks are coordinated throughout cardiac development remains an outstanding question in the field. Recent studies point to epigenetic modification as a potential mechanism for orchestrating cardiac development (Gregoire et al., 2013; Jung et al., 2005; Nakajima et al., 2011). Indeed, some epigenetic modifiers of heart development have been described, such as Brg1 of the BAF complex, the histone methyltransferase Jmjd3, and the histone deacetylase *hdac1* (Lickert et al., 2004; Lickert et al., 2004; Ohtani et al., 2013; Takeuchi et al., 2011; Song et al., 2019), but there likely remain many epigenetic regulators whose role in cardiogenesis has yet to be discovered.

The zebrafish *ugly duckling (udu)* locus, which encodes the evolutionarily conserved chromatin factor Gon4-like (Gon4l), was first identified for its effect on tail morphogenesis (Hammerschimidt et al., 1996; Liu et al., 2007). Subsequent work in zebrafish also defined roles for Gon4l in somitogenesis, and studies of both hypomorphic mouse *Gon4l* mutants and zygotic zebrafish *gon4l* mutants uncovered primitive erythroid cell deficiencies, which were attributed to abnormal cell cycle progression and increased TP53-mediated apoptosis. (Barr et al., 2017; Lim et al., 2009; Liu et al., 2007; Lu et al., 2010, 2011). Structural analysis of the murine Gon4l protein identified a putative SANT domain, which mediates interactions with Histone tails (Boyer, 2004). Previous studies also revealed a Yy1-binding domain (Liu et al., 2007; Lu et al., 2010), enabling interactions with the transcription factor Yy1, which acts as both a negative and positive regulator of gene expression (Deng, 2010; Gregoire et al., 2013). Additional work has demonstrated the ability of mouse Gon4l to bind Yy1 as well as HDAC1 (Lu et al., 2011), both of which are known epigenetic regulators of *nkx2.5* and have been implicated in heart development (Kook et al., 2003; Lu et al., 2011; Montgomery et al., 2007; Nambiar et al., 2007; Nan and Huang, 2009; Song et al., 2019).

Despite the importance of Gon4l in the development of mesoderm-derived tissues, including somites and blood (Lim et al., 2009; Liu et al., 2007; Williams et al., 2018) and in embryonic axis extension during gastrulation (Williams et al., 2018), the role of Gon4l in heart development has not been addressed. Here we show that Gon4l plays essential roles in patterning the cardiac chambers and regulating cardiomyocyte cell cycle during zebrafish heart development. Zygotic $udu^{-/-}$ mutant embryos exhibited mild defects in cardiac chamber morphogenesis and presented a slight reduction in the total number of cardiomyocytes at 24 hpf. Subsequently, the cardiomyocyte deficiency in $udu^{-/-}$ mutants became exacerbated due to reduced proliferation rather than the TP53-dependent apoptosis. We show that the proliferation defect was correlated with reduced expression of the G1/S-phase cell cycle regulator *cyclin E2* in $udu^{-/-}$ mutant hearts, and that the Gon4l protein associates with regulatory regions of the *ccne2* gene during early embryogenesis. Moreover, at 48 hpf $udu^{-/-}$ mutant hearts exhibited expansion of atrial cardiomyocytes at the expense of ventricular fate. Our studies further demonstrate that *udu* genetically interacts with *nkx2.5* to maintain the proportion of ventricular cardiomyocytes. Together, this work describes Gon4l as a novel modulator of heart development that regulates both cardiac chamber identity maintenance and proliferative processes.

2. Materials and methods

2.1. Zebrafish

Zebrafish were housed and handled according to protocols approved by the Institutional Animal Care and Use Committee of Washington University School of Medicine. AB* or AB*/Tubingen, Tg(*hsp70l:nkx2.5-eGFP*) (George et al., 2015), *Tg(myl7:GFP)* (Huang et al., 2003), udu^{vu66} (Williams et al., 2018), $nkx2.5^{vu179}$ (Targoff et al., 2013), $tp53^{zdf1}$ (Berghmans et al., 2005) were used. Fish were fed with rotifers during larval stages and rotifers and dry food during adulthood. Embryos were produced through natural matings, maintained at 28.5 °C, and staged according to Kimmel's embryonic stages (Kimmel, 1995).

2.2. Whole-mount in situ hybridization (WISH)

Embryos were fixed overnight in 4% paraformaldehyde (PFA) in phosphate buffered saline (PBS). Fixed embryos older than 24 hpf were bleached until pigment was removed in a solution containing 3% H_2O_2 and 0.5% KOH. WISH was performed as previously described using 65% formamide solution and 70 °C hybridization temperature (Thisse and Thisse, 2008). *Cardiac myosin light chain 7* (*myl7)* (Yelon et al., 1999), *atrial myosin heavy chain (myh6)* (Yelon et al., 1999) and *ventricular myosin heavy chain* (*myh7)* (Yelon et al., 2000) were used at 500 ng/μL, *nkx2.5* at 650 ng/μL (Chen and Fishman, 1996), *nkx2.7* at 150 ng/μL (Reifers et al., 2000). Stained embryos were cleared in 80% glycerol (Pradhan et al., 2017).

2.3. O-diansidine staining

Embryos were euthanized with 3-amino benzoic acidethylester (tricaine), and then placed in a mixture containing O-diansidine (0.06 g/mL), sodium acetate (0.01M, pH 4.5), hydrogen peroxide (0.65%) and 40% ethanol and incubated in the dark at room temperature for 15 min (mins) (Detreich et al., 1995). Stained embryos were cleared in 80% glycerol before imaging.

2.4. Heart dissection and DAPI labeling

Embryos were euthanized in tricaine, and hearts were manually extracted using 27G needles as previously described (Yang and Xu, 2012). Dissected hearts were fixed in 4% PFA for 20 min and then washed 3 times in PBS. Hearts were labeled with 2-(4-Amidinophenyl)-1H-indole-6-corboxamidine (DAPI) for 3 min and then washed twice with PBS before being mounted in 2% methylcellulose for imaging.

2.5. Immunohistochemistry

For anti-Caspase-3 antibody (Casp3, Cell Signaling, catalogue number:9661S) labeling, hearts were manually dissected as described

above and immunostained as previously described (Burns et al., 2005; Yang and Xu, 2012). Briefly, dissected hearts were fixed in 4% PFA, washed in PBT, and then blocked in 10% goat serum for 1 h at room temperature. The primary antibody was added (1:200) for 1 h, then the secondary antibody (Life Technologies, catalogue number: A11036) (1:400) for 30 min, both at room temperature. MF20 (Developmental Studies Hybridoma Bank, AB_2147781), S46 (Developmental Studies Hybridoma Bank, AB_528376) and Mef2 (Abcam, ab64644) labeling was performed in zebrafish embryos at 24 and 48 hpf (Alexander et al., 1998; Targoff et al., 2013). Embryos were euthanized in tricaine and then fixed for 1 h in 1% PFA in PBS, permeabilized for 1 h in 0.5% Triton-X100 and 10% goat serum in PBS. Embryos were incubated overnight in primary antibodies (1:20 for S40 and MF20, 1:200 for Mef2), then washed 3 times with PBS and incubated in secondary antibodies (Invitrogen, catalogue numbers: A21121, A21144, A21245) (1:200) for 2 h at room temperature.

2.6. EdU labeling

Embryos were placed in a 12.5% 5-ethynyl-2′-deoxyuridine (EdU), 7.5% dimethyl sulfoxide (DMSO) solution in 0.3X Danieau and incubated for 1 h on ice. Embryos were washed with 0.3X Danieau for 12 h at 28.5 °C (Just et al. 2016), and then euthanized with tricaine. Hearts were manually dissected and fixed for 20 min in 4% PFA (Yang and Xu, 2012). The dissected hearts were briefly rinsed 3 times with 3% bovine serum albumin (BSA) in PBS and then permeabilized for 30 min in 0.25% Triton-X100 and 1% DMSO in PBS. The hearts were then incubated for 30 min in the Click-It Reaction Buffer, washed 3 times in 3% BSA in phosphate buffer saline (PBT) and labeled with Mef2 antibody as described above.

3. TUNEL

TUNEL (terminal deoxynucleotidyl transferase biotin-dUTP nick end-labeling) was performed as previously described (Williams et al., 2018). Briefly, 48 hpf zebrafish embryos were fixed overnight in 4% PFA. Embryos were dehydrated using a series of methanol/PBT washes and stored at −20 °C at least overnight. Embryos were then rehydrated using a series of methanol/PBT solutions, permeabilized with proteinase K and ApopTag TUNEL (Millipore Sigma, Catalogue number: S7100) assay was performed according to the instructions provided.

3.1. Heat shock

Embryos obtained from natural crosses of *udu*$^{+/-}$;Tg(*hsp70l:nkx2.5-eGFP*)$^{+/-}$ to *udu*$^{+/-}$ (George et al., 2015) were maintained at 28.5 °C. At 21-somite stage, 50 embryos were transferred to 1.5 mL of embryo medium into a heat block held at 37 °C for 1 h. Transgenic embryos were identified by ubiquitous GFP expression. Non-transgenic siblings exposed to heat shock served as experimental controls.

3.2. Quantitative real-time (qRT) PCR

For total RNA extraction, 400–600 36 hpf Tg(*myl7:GFP*) transgenic embryos were euthanized using tricaine. Hearts were dissociated in L-15 media using gel loading pipette tips, and GFP fluorescence was used to manually isolate the population (Lombardo et al., 2015). The isolated hearts were briefly washed with L-15 media supplemented with 10% BSA and total RNA was extracted using Trizol (Ambion) with phenol/-chloroform extraction. cDNA was synthesized using the iScript Kit (BIO-RAD, catalogue number: 1708841) using 1,000 ng of RNA per 20 μL reaction. qRT-PCR was performed using SYBR green (Bio-Rad) using CFX Connect Real-Time machine with a minimum of three independent biological and technical samples. The following primers were used:

ccnd1 F: 5′-TGGGATCTGGCCTCAGTGAC-3’.
ccnd1 R: 5′-TGAAGTTGACGTCTGTCGCAC-3’.
ccnd2a F: 5′-AGCCGTATTAAAGGTCGAAAAGG-3’.
ccnd2a R: 5′-CCTCGCAGACCTCTAACATCCA-3’.
ccnd2b F: 5′-ACTGCTGTGGGAGTTGGTGG-3’.
ccnd2b R: 5′-AAGGTTTGCGTGTGCTTGCG-3’.
ccnd3 F: 5′-CATCGCCCTCACGGCTACAG-3’.
ccnd3 R: 5′-ACATGCAGAGAACGCCTTGTCC-3’.
ccne1 F: 5′-TCAGGGCTGAAGTGGTGTGA-3’.
ccne1 R: 5′-GGAGTGAACCTTTCCCAGCC-3’.
ccne2 F: 5′-GCACTGGACACTGCGGACAA-3’.
ccne2 R: 5′-GGGACTCTTCTATTGCACTCGCC-3’.
nkx2.5 F: 5′-CCGGATCCTCTCTTCAGCG-3’.
nkx2.5 R: 5′-CCTGACAAAACCCGATGTCTTT-3’.
nkx2.7 F: 5′-GCTTCAGTGTATGCAGAACACCC-3’.
nkx2.7 R: 5′-CGGGGCCGAAAGGTATCTCTGC-3’.

3.3. Genotyping

DNA was extracted from tricaine-euthanized whole embryos in a solution containing 10 mM Tris-HCL (pH 8), 50 mM KCL, 0.3% Tween-20, 0.3% NPA and 10 mg/mL proteinase K. Embryos subjected to WISH were treated with NaCl to reverse DNA crosslinking prior to DNA isolation (Gansner et al., 2008). The following primers were used:

udu^{vu66} F: 5′-GCACTTGCACAAACAGAGTTCCCGTA-3’.
udu^{vu66} R: 5′-CAAATTAACTACACGGGACAGCAAC-3’.
Followed by MaeIII digestion
p53^{zdf1} mutant F: 5′-AGCTGCATGGGGGGGAA-3’.
p53 WT F: 5′-AGCTGCATGGGGGAT-3’.
p53 R: 5′-GATAGCCTAGTGCGAGCACACTCTT-3’.
nkx2.5^{vu172} F: 5′-TTACCATCCCGAACCAAAAC-3’.
nkx2.5^{vu172} R: 5′-CAAACTCACCTCCACACAGG- 3’.
Followed by HinfI digest.
Tg*(hsp70l:nkx2.5-eGFP)* F: 5′-TCACCTCCACACAGGTGAAGATCTG-3’.
Tg*(hsp70l:nkx2.5-eGFP)* R: 5′-GGGTCAGCTTGCCGTAGGTGG-3’.

3.4. Image analysis

FIJI was used to visualize and manipulate all microscopy images. For dissected hearts labeled with Tg(*myl7:GFP*), DAPI, EdU, Caspase, Mef2, MF20 and S46, multiple Z-planes were imaged and projected to visualize the heart. Cardiomyocytes were manually counted in images of transgenic and immunostained embryos or hearts. Figures were prepared in Photoshop CS 6.

3.5. Statistical analysis

Statistical tests were conducted with GraphPad Prism v. 6. To compare the means of number of cardiomyocytes, proliferative index, apoptotic index and fold difference we used two-tailed, unpaired Student’s t-test and ANOVA. $p < 0.05$ was considered statistically significant (Table 1).

4. Results

4.1. Zygotic udu mutants exhibit diminutive hearts with a decreased proportion of ventricular cardiomyocytes

Although the nonsense *udu*^{vu66} allele in the zebrafish *ugly duckling/gon4l* locus was identified during a forward genetic screen as a recessive enhancer of shortened body axes in the non-canonical Wnt/Planar Cell Polarity (Wnt/PCP) mutant *gpc4/knypek (kny)* embryos (Williams et al., 2018), we observed that zygotic *udu*$^{vu66/vu66}$ (*udu* $^{-/-}$) mutants had small, dysmorphic hearts with severe edema at 48 h post fertilization (hpf) (Fig. 1A–D). Given the established roles of Gon4l in hematopoiesis and mesoderm development (Barr et al., 2017; Lim et al., 2009; Liu et al., 2007; Lu et al., 2010, 2011; Williams et al., 2018), we interrogated the functions of Gon4l in cardiogenesis.

Table 1
Key resources table.

Reagent or resource	Source	Identifier
Antibodies		
MF20	Developmental Studies Hybridoma Bank	AB_2147781
S46	Developmental Studies Hybridoma Bank	AB_528376
Mef2C	Abcam	Ab64644
Casp3	Cell Signaling	P42574 Cat#: 9661S
Bacterial and Virus Strains		
Biological Samples		
Chemicals, Peptides, and Recombinant Proteins		
o-Diansidine	Sigma	Cat#: D9143-5G
Critical Commercial Assays		
EdU Click-It Reaction Buffer	Thermo Fisher Scientific	Cat#: C10340
ApopTag Peroxidase In Situ Apoptosis Detection Kit	Millipore Sigma	Cat#: S7100
Deposited Data		
Experimental Models: Cell Lines		
Experimental Models: Organisms/Strains		
udu^{vu66}	Williams et al. (2018)	N/A
Tg(*cmlc2:GFP*)	Huang et al. (2003)	ZDB-ALT-060719-2
Tg(*hsp70l:nkx2.5-eGFP*)	George et al. (2015)	ZDB-TGCONSTRCT-150527-1
nkx2.5^{vu179}	Targoff et al. (2013)	ZDB-ALT-131212-1
tp53^{zdf1}	Berghmans et al. (2005)	ZDB-ALT-050428-2
Oligonucleotides		
Primers for qRT-PCR: *cnne1, cnne2, cnnd1, cnnd2a, cnnd2b, cnnd3, nkx2.5, nkx2.7, gapdh* See Supplemental Table S1	Liu et al., 2017 Targoff et al. (2008)	N/A
Primers for genotyping *udu*^{vu66}, Tg(*hsp70l:nkx2.5-eGFP*), *nkx2.5*^{vu179}, *tp53*^{zdf1} See Supplemental Table S2	Williams et al. (2018) Targoff et al. (2013) Berghmans et al. (2005)	N/A
Recombinant DNA		
Software and Algorithms		
Other		

To characterize cardiac development in *udu*$^{-/-}$ mutants, we first performed whole mount in situ hybridization (WISH) for the cardiac markers *myosin light chain 7* (*myl7)* (which labels the entire myocardium) (Yelon et al., 1999), *myosin heavy chain 6 (myh6)* (atrium) (Yelon et al., 1999) and *myosin heavy chain* 7 (*myh7)* (ventricle) (Yelon et al., 2000) in 24 hpf embryos to examine overall heart tube morphology and initial patterning of the atrium and ventricle (Fig. 1 E-G, H-J). Unlike wild-type (WT) embryos, in which the heart tube extended toward the left eye (n = 19/24), the majority of *udu*−/− heart tubes did not fully extend (n = 19/21) (Fig. 1 E, H). Moreover, the expression patterns of *myh6* (n = 15/16) and *myh7* (n = 11/12) highlighted the abnormal shapes of the atrial and ventricular chambers in *udu*−/− embryos (Fig. 1I and J) compared to WT (F, G).

Next, we asked how the zygotic loss of *udu/gon4l* function affects heart development after heart tube formation. To this end, we performed WISH for *myl7, myh6* and *myh7* in *udu*$^{-/-}$ embryos at 48 hpf and found that the domain of *myl7* expression was reduced, with both the atrium and ventricle being affected. We observed that at this stage, expression domains of *myl7, myh6* and *myh7* were smaller in almost all *udu*−/− mutants (Fig. 1 N, O, P) (n = 37/38, n = 30/32, n = 40/41) compared to WT embryos (Fig. 1 K, L, M) (n = 38/40, n = 48/50, n = 41/41). To quantify these defects, we performed immunofluorescent (IF) staining of WT and *udu*−/− hearts using antibodies that label the atrial myocardium and the entire heart (S46 and MF20, respectively) together with the pan-cardiomyocyte nuclear marker Mef2 (Ticho et al., 1996; Yelon et al., 1999), followed by fluorescent confocal microscopy to visualize morphology of the cardiac chambers. Ventricular myocardium is indicated by MF20 IF labeling in the absence of S46 signal (MF20^{+}S46^{-}). At 24 hpf, we found a decrease in the total number of cardiomyocytes in *udu*$^{-/-}$ embryos (105 ± 4.6, n = 16) relative to WT (130 ± 3.1, n = 13) (Fig. 2A and B, E). Moreover, the proportion of cardiomyocytes with MF20^{+}S46^{-} antibody labeling was not significantly different between WT (53 ± 2.0%, n = 11) and *udu*$^{-/-}$ (47 ± 3.0%, n = 12) embryos (p = 0.14) (Fig. 2 F). Quantification revealed that the total number of cardiomyocytes with ventricular identity was higher in WT (69 ± 3.3, n = 13) than in *udu*$^{-/-}$ mutant embryos (50 ± 4.0, n = 16). As suggested by the smaller overall heart size, the number of cardiomyocytes expressing atrial identity was also higher in WT embryos (62 ± 3.0, n = 13) than in *udu*$^{-/-}$ mutant embryos (55 ± 3.4, n = 16). Taken together, our data suggests that, at 24 hpf, *udu*$^{-/-}$ mutants possess smaller hearts but with normal proportions of ventricular and atrial cardiomyocytes.

Such confocal IF microscopy experiments carried out at 48 hpf revealed that the reduction in cardiomyocyte number was greatly exacerbated, with WT embryos containing approximately twice the number of cardiomyocytes (204 ± 4.9, n = 13) as *udu*−/− mutants (108 ± 5.8, n = 16) (p = 0.0001) (Fig. 2C and D, E). Notably, there was no significant increase in the number of cardiomyocytes in *udu*−/− embryos between 24 hpf (105 ± 4.6) and 48 hpf (108 ± 5.8) (p = 0.70), suggesting that the cardiomyocyte population did not expand after 24 hpf in the mutant embryos. In contrast to the static cardiomyocyte population in *udu*$^{-/-}$ embryos, the cardiomyocyte population in WT embryos increased by more than 50 percent between 24 and 48 hpf (Fig. 2 E), consistent with previous reports (Bennett et al., 2013). We also found that the proportion of ventricular cardiomyocytes (MF20+/S46-) was reduced in *udu*−/− hearts (41 ± 2.0, n = 16) relative to WT (59 ± 1.0, n = 13) (p = 0.0009) (Fig. 2 F). The total number of cardiomyocytes with ventricular identity was higher in WT (102 ± 2.9, n = 13) than in *udu*$^{-/-}$ mutant embryos (44 ± 3.7, n = 16). As suggested by the smaller overall heart size, the number of cardiomyocytes expressing atrial identity was also higher in WT embryos (102 ± 3.6, n = 13) than in *udu*$^{-/-}$ mutant embryos (64 ± 3.8, n = 16). Together, these findings suggest that *udu* expression is required for the maintenance of proper proportions of ventricular cardiomyocytes, and that *udu* expression is also required for expansion of the cardiomyocyte population between 24 and 48 hpf, likely through either reducing apoptosis or by increasing proliferation.

4.2. TP53-mediated cell death is not responsible for the reduced cardiomyocyte numbers in udu mutants

Zygotic loss of *udu/gon4l* function has been shown to increase *tumor protein 53* (*tp53)* expression and consequently apoptosis in the 24 hpf zebrafish embryo resulting in erythropoietic deficiencies (Lim et al., 2009; Liu et al., 2007). Accordingly, it was found that reducing *tp53* expression using an antisense morpholino oligonucleotide (MO) partially restored blood development in *udu*$^{-/-}$ mutants at 48 hpf (Liu et al., 2007). We observed that embryos homozygous for the *udu*^{vu66} allele also exhibited increased cell death (Fig. 1S A, B) and blood deficiencies (Fig. 2S A, B) observed previously in the zygotic *udu*$^{sq1/sq1}$ mutants at 24 hpf (Liu et al., 2007). Considering that cardiomyocytes and blood share a developmental origin in the LPM (Kimelman, 2006), we hypothesized that the mechanism underlying the cardiomyocyte deficiency in *udu*−/− embryos could represent the same defect responsible for impaired blood development. Therefore, we tested whether inhibition of TP53-mediated apoptosis would also restore cardiomyocyte number in *udu*−/− embryos (Van Vliet et al., 2012).

To this end, we generated *udu*$^{-/-}$*;tp53*$^{zdf1/zdf1}$ double mutant zebrafish embryos. To first establish that we could reproduce the results obtained using a *tp53* MO, we examined these compound mutants for restoration of blood development by staining for hemoglobin using O-

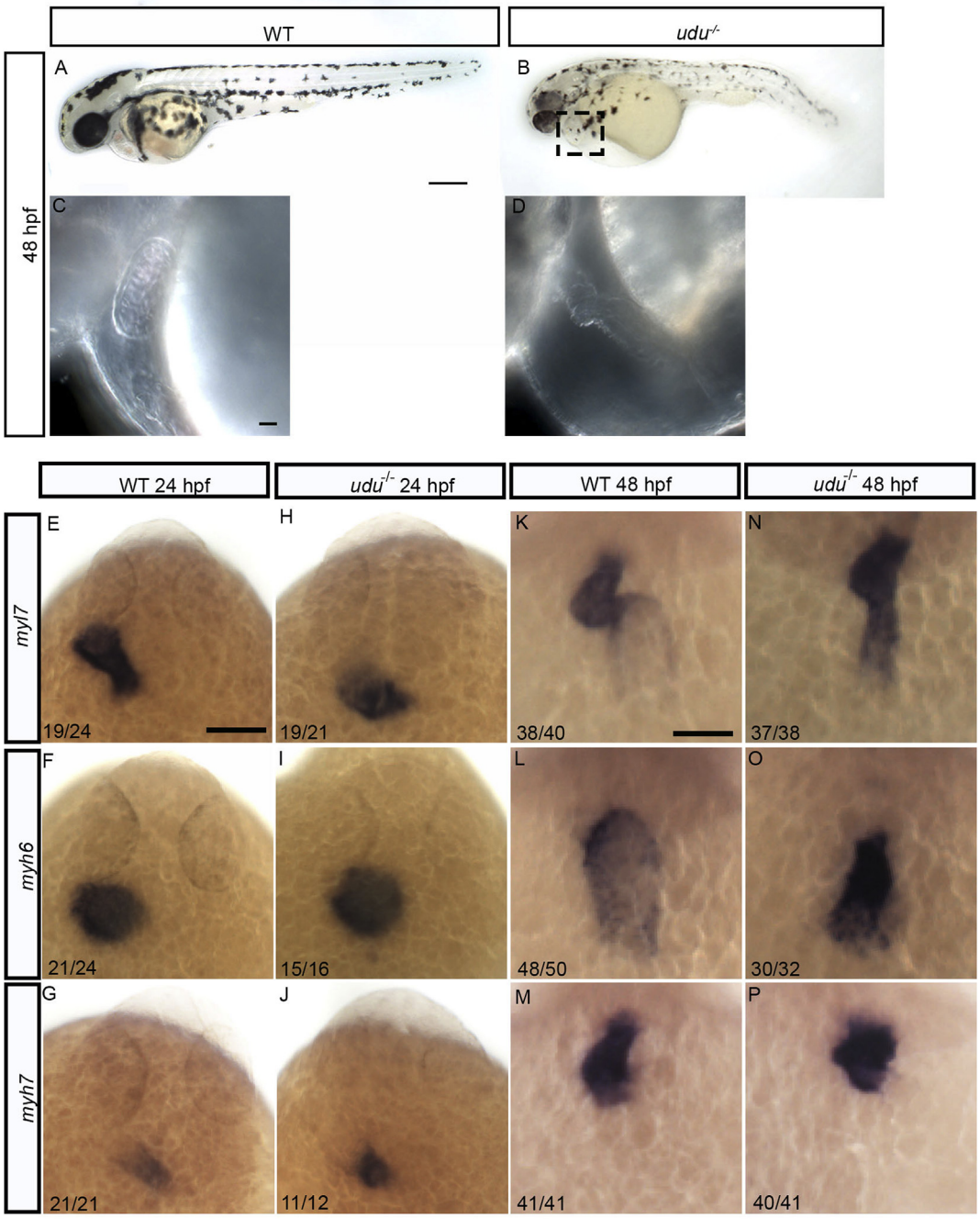

Fig. 1. Loss of zygotic Gon4l function affects cardiac chamber patterning and causes a reduction in number of cardiomyocytes. Lateral view of WT embryos (A) and *udu*$^{-/-}$ (B) and their heart region (C, D) at 48 hpf. Dorsal view of WT (E, F, G) and *udu*$^{-/-}$ embryos (H, I,J) showing the expression of *myl7 (E, H), myh6 (F, I),* and *myh7* (G, J) at 24 hpf by WISH. Dorsal view of *myl7 (K, N), myh6 (L, O),* and *myh7* (M, P) expression at 48 hpf by WISH in WT (K, L, M) *udu*$^{-/-}$ (N, O, P) embryos.

diansidine at 48 hpf (Berghmans et al., 2005). *udu*−/− embryos with loss of zygotic *tp53* expression exhibited no O-diansidine staining, indicating an absence of erythroid cells (Fig. 2S C) (n = 17/18) comparable to that observed in single *udu*−/− mutants (Fig. 2S B). These experiments indicated that zygotic loss of *tp53* was not sufficient to suppress the blood development deficiency in zygotic *udu* mutants. However, the *tp53* morpholino studies described above were conducted with a translation-blocking *p53* MO that likely disrupts both maternal and zygotic *tp53* function (Liu et al., 2007). Hence, we next tested if maternal and zygotic (MZ) loss of *tp53* could recapitulate the previously described suppression of blood deficiency phenotype in *udu*$^{-/-}$ embryos (Liu et al., 2007), by crossing *udu*$^{+/-}$;*tp53*$^{-/-}$ female to *udu*$^{+/-}$;*tp53*$^{+/-}$ male fish. O-diansidine staining of the resulting embryos followed by genotyping demonstrated that the majority (n = 34/44) of *udu*$^{-/-}$;MZ*tp53*$^{-/-}$ embryos displayed a partial restoration of blood development (Fig. 2S D). This finding verified the earlier morpholino study, which demonstrated that reduced hematopoiesis in *udu*$^{-/-}$ mutant embryos is largely dependent on TP53 function (Liu et al., 2007).

Having confirmed *tp53* and *udu* genetically interact in blood development, we next asked if loss of zygotic or maternal and zygotic *tp53* function would increase the number of cardiomyocytes in *udu*−/− embryos at 48 hpf. Using the Tg(*myl7:GFP*) transgenic line to visualize cardiomyocytes with GFP expression and DAPI to label nuclei, we quantified cardiomyocyte number in confocal images of hearts isolated from WT, *udu*$^{-/-}$, *udu*$^{-/-}$;Z*tp53*$^{-/-}$; and *udu*$^{-/-}$; MZ*tp53*$^{-/-}$ mutant embryos (Fig. 2S E-H, K). We found that zygotic loss of *tp53* in *udu*$^{-/-}$

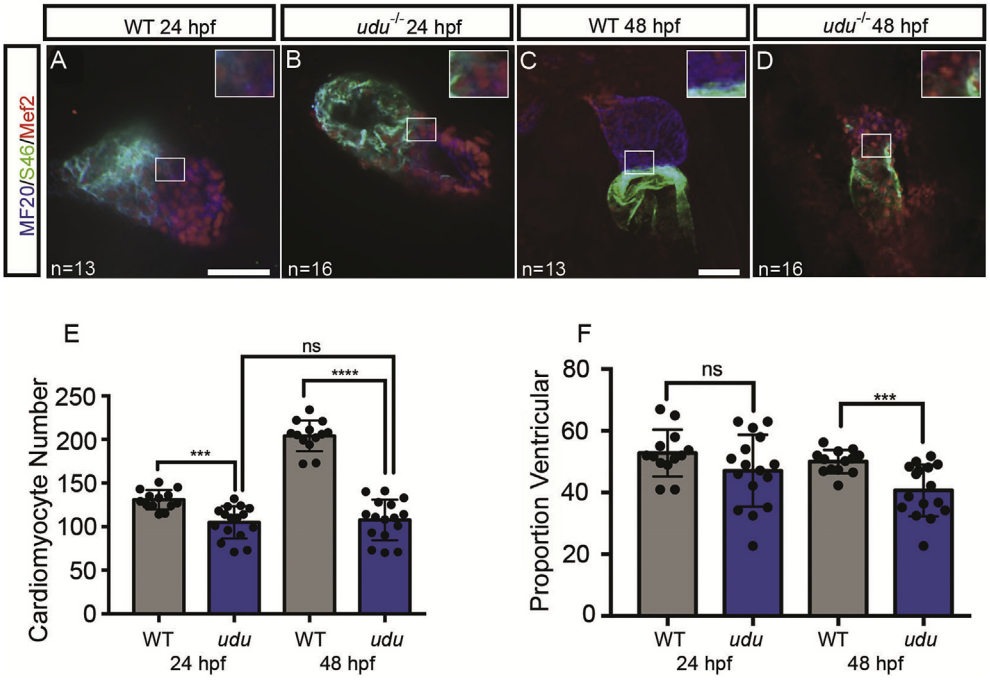

Fig. 2. Loss of zygotic Gon4l function affects cardiac chamber patterning after heart tube formation and results in a reduction in the number of cardiomyocytes. Immunofluorescence confocal images of cardiac chambers at 24 hpf using MF20 (blue, myocardium) and S46 (green, atrium) and Mef2 (red, cardiomyocyte nuclei) antibodies to mark the cardiac chambers in WT (A, C) and *udu*−/− mutant (B, D) embryos at 24 hpf (A, B) and 48 hpf (C, D). Cardiomyocyte number (E) and percentage of total cardiomyocytes with ventricular identity (F) at 24 hpf and 48 hpf in WT (grey) and *udu*−/− mutant (blue) embryos. *$p < 0.05$, **$p < 0.01$, ***$p < 0.001$, ****$p < 0.0001$, error bars = SEM. Scale bars represent 50 μm. Inserts show a 2X magnification from images.

embryos did not significantly increase cardiomyocyte number (118 ± 7; n = 11) (mean ± SEM) compared with *udu*$^{-/-}$ hearts with functional *tp53* expression (115 ± 6; n = 33) (p = 0.84) (Fig. 2S F, G, K). This result indicates that zygotic loss of *tp53* is not sufficient to suppress the cardiomyocyte deficiency in *udu*$^{-/-}$ embryos. Surprisingly, we found that *udu*$^{-/-}$;MZ*tp53*$^{-/-}$compound mutant embryos also had a similar number of cardiomyocytes (107 ± 6; n = 13) as single *udu*$^{-/-}$ mutants (115 ± 6; n = 33) (p = 0.41) (Fig. 2S F, H, K). This indicates that despite restoring blood development, loss of maternal and zygotic *tp53* function failed to restore cardiomyocyte numbers in *udu*$^{-/-}$ embryos (Fig. 2S K). Together, these results demonstrate that the cardiomyocyte deficiency in *udu*$^{-/-}$ mutant embryos is not caused by *tp53*-dependent apoptosis.

To further corroborate this finding, we assayed the number of apoptotic cells in WT and *udu*$^{-/-}$ mutant embryos at 48 hpf using immunofluorescent labeling for activated Caspase 3 (Casp3+) (Fig. 2S I, J) and found that there was no significant increase in apoptosis of *udu*$^{-/-}$ mutant cardiomyocytes (0.58 ± 0.22; n = 18) relative to WT (0.34 ± 0.13; n = 18) (p = 0.37) (Fig. 2S L). Likewise, TUNEL staining in the embryonic hearts revealed that the vast majority of both WT (Fig. 1S C) (n = 19/21) and *udu*$^{-/-}$ mutant hearts (Fig. 1S D) (n = 28/30) contained no TUNEL-postive cells.

Altogether, these data indicate that increased cell death is not responsible for the reduced number of cardiomyocytes observed in *udu*$^{-/-}$ mutant embryos. These findings suggest that the mechanism by which Gon4l modulates the number of cardiomyocytes is distinct from its role in hematopoiesis despite their common developmental origin. Furthermore, these results indicate a broader role for Gon4l in the development of mesoderm-derived tissues beyond its function in suppressing apoptosis.

4.3. *Cardiomyocyte proliferation is reduced in udu mutants*

Proliferation is essential for expansion of the cardiomyocyte population following heart tube formation (Leone et al., 2015; Rohr et al., 2006). Based on our finding that the number of cardiomyocytes in *udu*$^{-/-}$ embryos is static between 24 and 48 hpf despite a near doubling of WT cardiomyocytes (Fig. 2 E), we examined whether the proliferation rate of cardiomyocytes was affected in *udu*$^{-/-}$ embryos. To this end, we employed EdU incorporation for 1 h in 36 hpf embryos to label cardiomyocytes that progress through S-phase of the cell cycle (Fig. 3 A) (Salic and Mitchison, 2008). We co-labeled cardiomyocyte nuclei with the Mef2 antibody and quantified the number of EdU/Mef2 double-positive cells in confocal images of the isolated labeled hearts.

We first determined that the proliferative index – the percent of cardiomyocytes that incorporated EdU – was 2.6 ± 0.35% (Fig. 3 B, D white arrow) (n = 13) in WT hearts compared with 0.59 ± 0.2% (n = 18) (Fig. 3C and D) of *udu*$^{-/-}$ cardiomyocytes at 36 hpf. This result suggests that relative to the cardiomyocytes in WT, the cardiomyocytes in *udu*−/− embryos have a reduced capacity to progress through S-phase of the cell cycle ($p < 0.0001$). Non-cardiomyocyte heart cells also exhibited reduced proliferation, as the presumed endocardium (non-Mef2 positive cells lining the cardiomyocytes) of *udu*−/− hearts contained fewer EdU + cells than WT endocardium (Fig. 3 B–C, green arrow).

These results indicate that cardiomyocyte proliferation is reduced in *udu*$^{-/-}$ mutant embryos, implicating a failure of cell cycle progression. Previous studies found that the expression levels of cell cycle regulators *Cyclin D (Cnnd3)* and *Cyclin E2* (*Cnne2*) were reduced in multipotent hematopoietic progenitors isolated from *Gon4l* hypomorphic mutant mice (Barr et al., 2017). To test if cell cycle genes are similarly misregulated in *udu*−/− zebrafish hearts, we measured the abundance of transcripts encoding the D and E type Cyclin-encoding genes in WT and *udu*$^{-/-}$ mutant hearts at 36 hpf, including: *ccnd1, ccnd2a, ccnd2b, ccnd3, cnne1,* and *cnne2* by qRT-PCR. This analysis revealed that levels of *cnnd1, ccnd2a, ccnd2b,* and *ccne1* transcripts (Fig. 3E and F, G, I) were unchanged at this stage ($p > 0.05$), but two Cyclin-encoding genes were differentially expressed in the *udu*$^{-/-}$ mutant embryo hearts. Whereas expression level of the early G1-stage Cyclin-encoding gene *ccnd3* was significantly increased in *udu* mutant embryo hearts compared to WT (p = 0.016) (Fig. 3 H), the expression of *cnne2* was significantly reduced in the *udu*$^{-/-}$ mutant hearts relative to WT (p = 0.001) (Fig. 3 J). Because *cnne2* expression peaks at the G1/S phase transition and is required for entry into S-phase (Siu et al., 2012), these results corroborate our finding that EdU incorporation was reduced in *udu*$^{-/-}$ mutant embryos (Fig. 3 D). Ccnd3 is essential for regulating erythroid cell proliferation in mice and mediates progression through the G1/S-phase check-point; the function of Ccnd3 in the cell-cycle of non-erythroid cells is not known (Sankaran et al., 2012). The differential expression of *ccnd3* and *ccne2* indicates that Gon4l may mediate cardiomyocyte progression through the cell cycle via regulation of Cyclin gene expression.

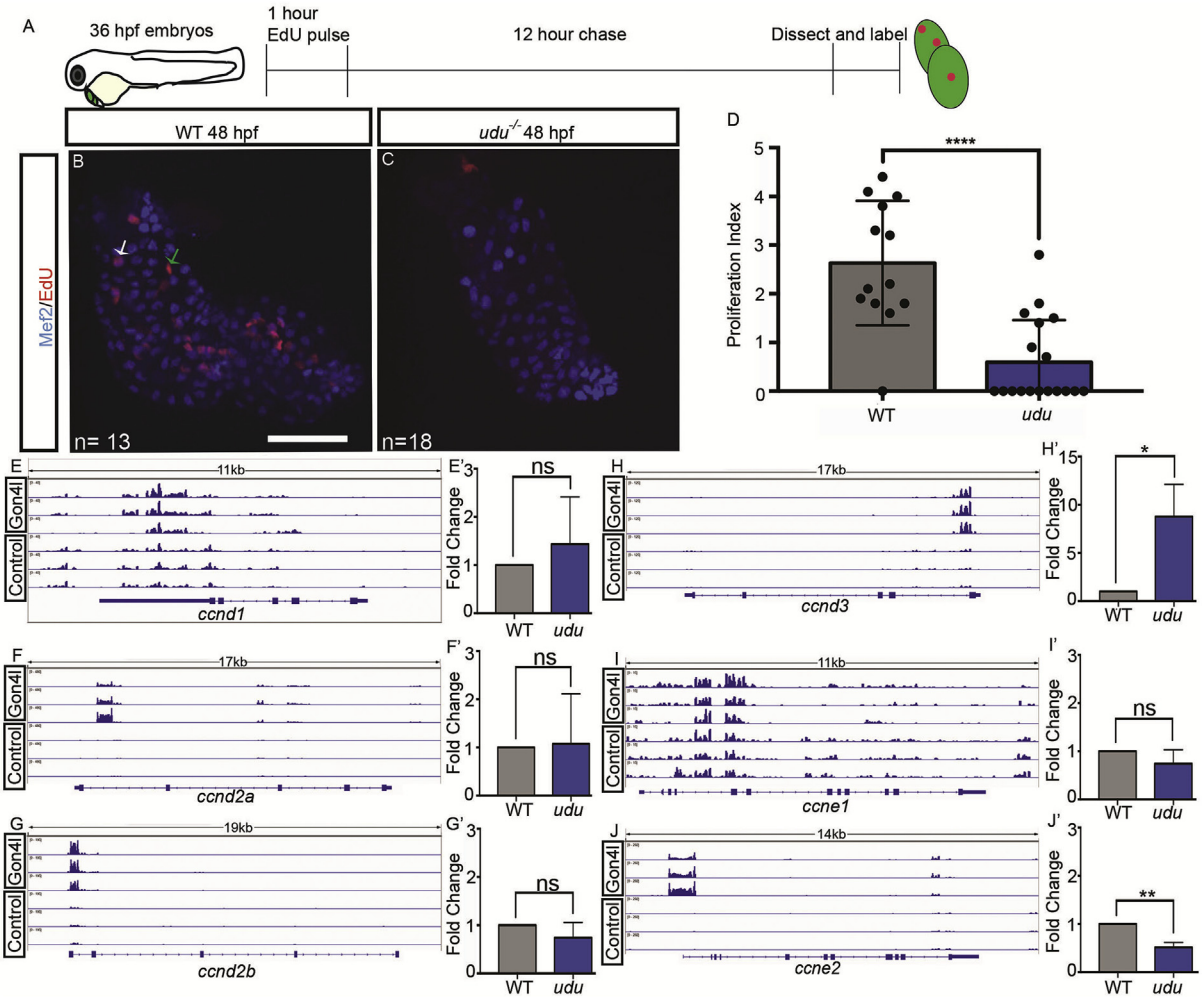

Fig. 3. EdU incorporation is reduced in the hearts of *udu*$^{-/-}$ embryos. Experimental workflow for EdU labeling (A). EdU labeling (red) in 48 hpf WT hearts (B) and *udu*−/− hearts (C) with cardiomyocytes labeled by Mef2 (blue). Arrows showing EdU + cardiomyocyte (white) and non-cardiomyocyte (green). Graph showing the proliferative index for EdU in WT (grey) and *udu*−/−(blue) cardiomyocytes (D). qRT-PCR for *ccnd1* (E), *ccnd2a* (F), *ccnd2b* (G), *ccnd3* (H), *ccne1* (I), and *ccne2* (J) performed on RNA extracted from hearts isolated from 36 hpf WT (grey) and *udu*−/−(blue) embryos. Results are shown as fold change of gene expression in *udu*−/− embryos compared to WT and results were standardized to *gapdh* expression. DamID-seq Genome browser tracks of Gon4l-Dam and GFP Control-Dam at *ccnd1* (E′), *ccnd2a* (F′), *ccnd2b* (G′), *ccnd3* (H′), *ccne1* (I′), and *ccne2* (J′) loci. *p < 0.05, **p < 0.01, ***p < 0.001, ****p < 0.0001, error bars = SEM. Scale bar represents 50 μm.

We next analyzed our group's previously published DNA adenine methyltransferase identification with sequencing (DamID-seq) data to determine whether D and E type Cyclin genes are direct targets of Gon4l regulation. This technique employs a Gon4l-methyltransferase fusion protein to identify regions of the genome with which Gon4l associates (Steensel, 2001; Williams et al., 2018). Our analysis found that at tailbud stage (the end of gastrulation), Gon4l association was enriched at regions near *ccnd2a, ccnd2b, ccnd3*, and *cnne2* (Fig. 3 F′-H′, J′), suggesting that Gon4l may directly regulate the expression of these *cyclins*. One caveat is that these DamID-Seq data are from whole gastrulae at tailbud stage, and thus may not accurately reflect Gon4l association in a specific cell type and at later stages. Nevertheless, these DamID-Seq data together with our qRT-PCR and EdU results indicate a potential role for Gon4l in mediating progression into S-phase through regulating expression of G1/S phase cyclins.

4.4. Expression of *nkx2.5* and *nkx2.7* is reduced in *udu*$^{-/-}$ mutants following heart tube formation

Studies in zebrafish have defined two distinct phases of cardiomyocyte development. First, the primary heart field is specified in bilateral regions of the ALPM during early segmentation. Then, after heart tube formation, the second heart field extends the two poles of the heart tube and contributes to the development of the two cardiac chambers (Buckingham et al., 2005; Cai, 2003; De La Cruz, 1977; Dominguez et al., 2012; Dyer and Kirby, 2009; Galli et al., 2008; Rana et al., 2014; Vincent and Buckingham, 2010; Zaffran, 2002; Zaffran et al., 2004). The transcription factors Nkx2.5 and Nkx2.7 play critical roles in the regulation of both the primary and second heart fields and are necessary for maintenance of ventricular identity in zebrafish embryos (George et al., 2015; Targoff et al., 2008, 2013).

Given that previous studies in mouse embryonic stem cells suggest that *nkx2.5* expression can be regulated by the Gon4l binding partner Yy1 (Gregoire et al., 2013; Lu et al., 2011), and the established role of Nkx2.5 in patterning heart chambers and maintaining ventricular fate (Gregoire et al., 2013; Lu et al., 2011; Targoff et al., 2008, 2013), we next examined expression of *nkx2.5* (Fig. 4A–F) and *nkx2.7* (Fig. 4G–L) by WISH in *udu*$^{-/-}$ mutant and WT embryos during late segmentation stages through heart tube formation. During cardiomyocyte precursor specification at the 12-somite stage, the majority of both WT and *udu*$^{-/-}$ embryos presented normal bilateral expression domains of *nkx2.5* and *nkx2.7* in the ALPM (Fig. 4A and B, G, H). Likewise, at the 16-somite stage, *nkx2.5* and *nkx2.7* were expressed in comparable domains in WT and *udu*$^{-/-}$ mutant embryos (Fig. 4C and D, I, J).

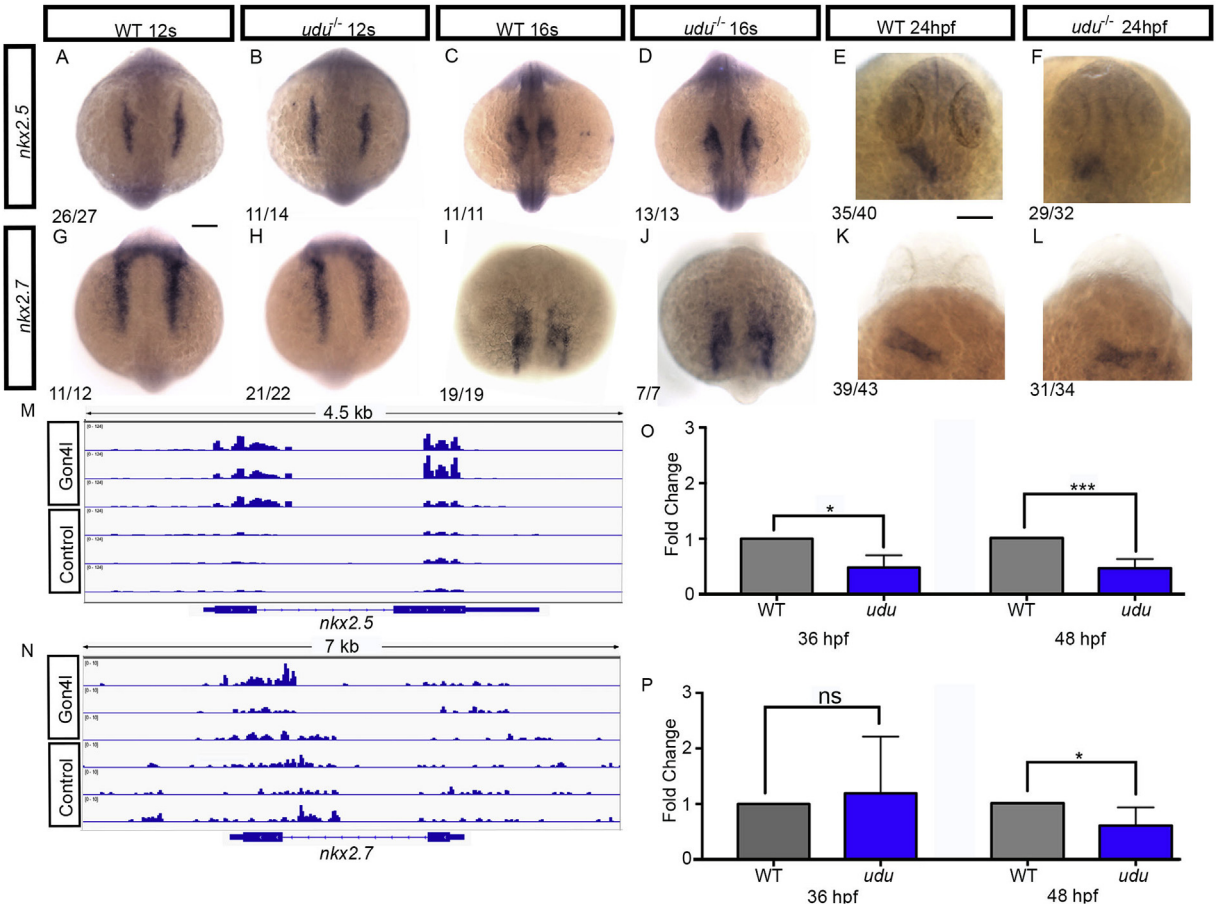

Fig. 4. Expression of *nkx2.5* and *nkx2.7* is initiated normally in the nascent cardiomyocytes of *udu*$^{-/-}$ embryos, but becomes reduced following heart tube formation. Dorsal view of embryos showing expression of *nkx2.5* (A–F) and *nkx2.7* (G–L) detected by WISH in WT (A, C, E, G, I, K) and *udu*$^{-/-}$ (B, D, F, H, J, L) embryos at 12 somites (A, B, G, H), 16 somites (C, D, I, J) and 24 hpf (E, F, K, L) stages. DamID-seq Genome browser tracks of Gon4l-Dam and GFP Control-Dam at *nkx2.5* (M) and *nkx2.7* (N) loci. Graph of qRT-PCR results performed on RNA extracted from hearts isolated from 36 hpf and 48 hpf WT and *udu*$^{-/-}$ embryos for *nkx2.5* (O) and *nkx2.7* (P) expression; results were standardized to *gapdh* expression. *p < 0.05, **p < 0.01, ***p < 0.001, ****p < 0.0001, error bars = SEM. Scale bars represent 50 μm.

However, during cardiac chamber patterning at 24 hpf, *nkx2.5* (Fig. 4E and F) and *nkx2.7* (Fig. 4K and L) genes exhibited expression domains that appeared to be smaller in size in *udu*$^{-/-}$ mutant embryos compared to WT. To assess whether the differences in expression domains could reflect changes in gene expression levels, we performed qRT-PCR on RNA isolated from hearts of WT and *udu* mutant embryos at 36 and 48 hpf. These qRT-PCR experiments revealed that at 36 hpf, expression of *nkx2.5* (Fig. 4 O) ($p = 0.02$), but not *nkx2.7* ($p = 0.72$) (Fig. 4 P), was significantly reduced *udu*$^{-/-}$ mutant hearts compared to WT. By contrast, heart-specific qRT-PCR analyses at 48 hpf found that expression levels of both *nkx2.5* ($p = 0.0006$) and *nkx2.7* ($p = 0.05$) were significantly decreased in *udu*$^{-/-}$ mutants (Fig. 4 O, P).

We again revisited zebrafish DamID-Seq datasets that mapped the genomic occupancy of Gon4l at the tailbud stage (Williams et al., 2018), to determine whether either of these genes could be a direct target of Gon4l regulation. We observed an enrichment of Gon4l association near *nkx2.5* (Fig. 4 M) but not *nkx2.7* (Fig. 4 N). The murine Gon4l is known to bind Yy1 (Lu et al., 2011), which was previously shown to associate with a cardiac-specific *Nkx2.5* enhancer (Gregoire, 2013). However, these zebrafish DamID-Seq data place Gon4l at the *nkx2.5* locus, supporting a potentially primary role for Gon4l in regulating expression of this cardiac transcription factor, likely via interactions with Yy1 and/or other DNA binding proteins. Based on these results we propose that Gon4l is involved in maintaining *nkx2.5* expression during heart tube formation and cardiac chamber patterning.

4.5. *udu* genetically interacts with nkx2.5 to maintain ventricular identity

Nkx2.5 is a key regulator of ventricular fate (Targoff et al., 2008, 2013; Tu et al., 2009). Considering the reduced expression of *nkx2.5* in *udu*$^{-/-}$ mutant embryos post-heart tube formation (Fig. 4 O), the reduced number of ventricular cardiomyocytes observed in these embryos (Fig. 2C and D, F), we hypothesized that *udu* maintains ventricular fate through interactions with *nkx2.5*. We therefore tested for genetic interaction between *udu* and *nkx2.5* by examining cardiac chamber patterning in the progeny of *nkx2.5*$^{+/-}$;*udu* $^{+/-}$ double heterozygotes using antibodies S46 and MF20 to label the cardiac chambers (Fig. 5 A). We noted that compared to both *udu*$^{-/-}$ (Fig. 5 B) and *nkx2.5*$^{-/-}$ (Fig. 5 C) *nkx2.5*$^{-/-}$;*udu*$^{-/-}$ (Fig. 5 D) double mutant embryos appeared to have a more severe reduction of the ventricle than either single mutant.

We further characterized this genetic interaction between *nkx2.5* and *udu* using antibody labeling for Mef2, MF20, and S26 (as described above) to quantify the number of atrial and ventricular cardiomyocytes (Fig. 5 E). We found that the percentage of ventricular cardiomyocytes was significantly reduced in both *udu*$^{-/-}$ (40 ± 1.4, $n = 30$) ($p = 0.036$) (Fig. 5 B) and *nkx2.5*$^{-/-}$ embryos (28 ± 1.7, $n = 13$) ($p < 0.0001$) (Fig. 5 C) single mutant embryos relative to WT (48 ± 1.8, $n = 12$) (Fig. 5 A, E). We then examined hearts from *nkx2.5*$^{-/-}$; *udu*$^{-/-}$ double mutants, and observed an almost complete absence of ventricular cardiomyocytes, with nearly the entire heart comprised of atrial cardiomyocytes (Fig. 5 D). Accordingly, our quantifications of ventricular cardiomyocytes

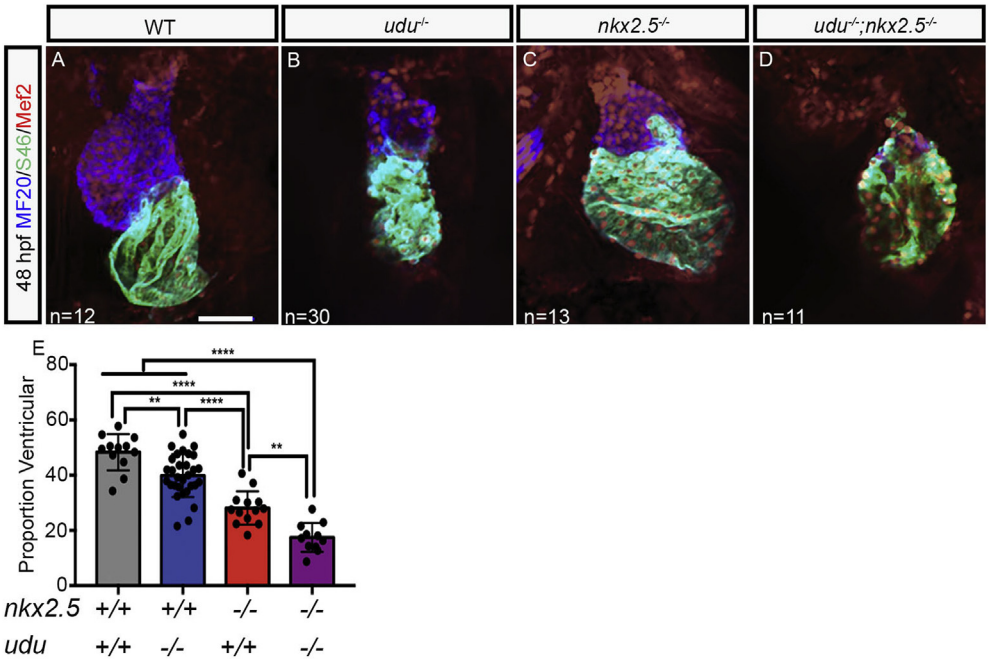

Fig. 5. *udu* genetically interacts with *nkx2.5* to maintain ventricular identity. Confocal immunofluorescence images of ventral views of WT (A), *udu*−/− (B), *nkx2.5*$^{-/-}$ (C), and *udu*−/−; *nkx2.5*$^{-/-}$(D) zebrafish hearts at 48 hpf with showing the myocardium (MF20, blue) and atrium, (S46, green), and nuclei of cardiomyocytes (Mef2, red). Proportion of total cardiomyocytes with ventricular identity at 48 hpf in WT (grey), *udu*−/−;nkx2.5$^{+/+}$ (blue) *udu*$^{+/+}$*;nkx2.5*$^{-/-}$ (red) and *udu*$^{-/-}$*;nkx2.5*$^{-/-}$ (purple) embryos (E). *p < 0.05, **p < 0.01, ***p < 0.001, ****p < 0.0001, error bars = SEM. Scale bars represent 50 μm.

revealed that *nkx2.5*$^{-/-}$*; udu*$^{-/-}$ (Fig. 5 E) double mutants showed a more severe reduction in the percentage of ventricular cardiomyocytes (17 ± 1.6, n = 11) compared to either *udu*$^{-/-}$ (40 ± 1.4, n = 30) (p < 0.0001) or *nkx2.5*$^{-/-}$ (28 ± 1.7, n = 13) (p = 0.002) single mutants (Fig. 5 E). *nkx2.5*$^{-/-}$ mutants displayed a reduction in the total number of cardiomyocytes with ventricular identity (50 ± 3.5, n = 13) relative to WT (94.6 ± 9.2, n = 12). Likewise, *udu*−/− (41.7 ± 2.5, n = 30) single mutants and *nkx2.5*$^{-/-}$*; udu*$^{-/-}$ double mutants (17.4 ± 2.1, n = 11) also had fewer cardiomyocytes with ventricular identity than WT embryos.

Heterozygous loss of neither *nkx2.5* nor *udu* affected cardiac chamber patterning in WT or *nkx2.5*$^{-/-}$ or *udu*$^{-/-}$ mutant backgrounds (Fig. 3S A-D, F, H, J). This suggests that the interaction is not dose-dependent and that loss of a single copy of *nkx2.5* or *udu* is not sufficient to perturb cardiac chamber patterning. Taken together, these results intimate that

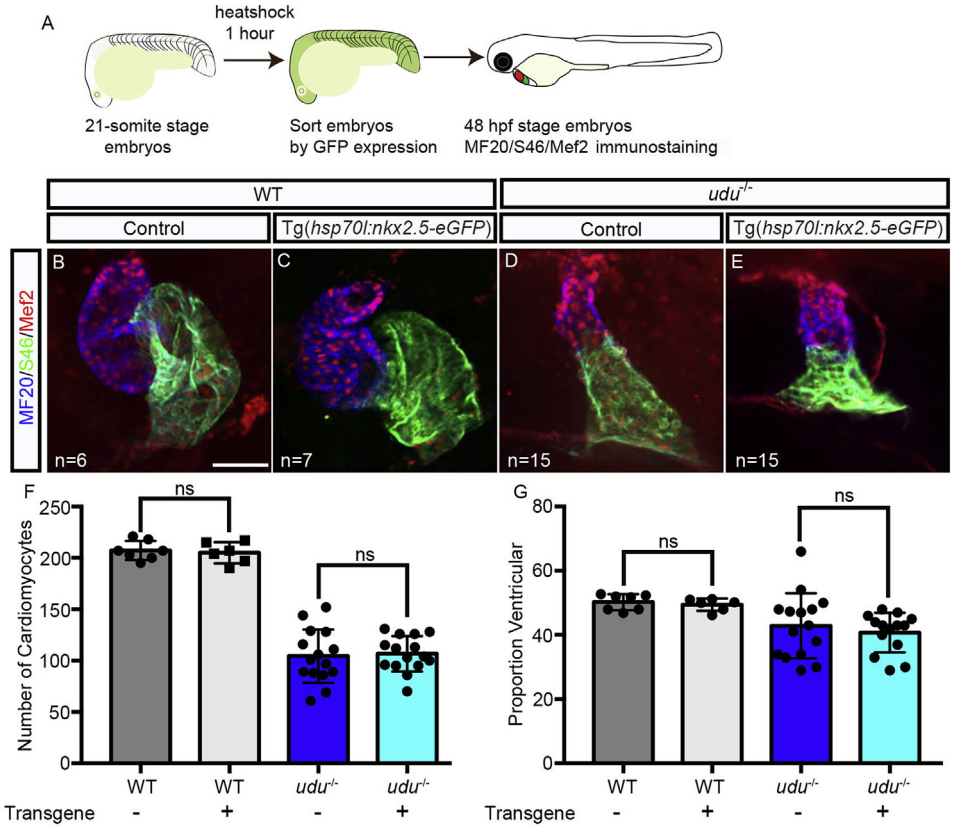

Fig. 6. Ectopic *nkx2.5* expression is not sufficient to rescue ventricular identity in *udu*$^{-/-}$ embryos. Experimental workflow (A). Immunofluorescent labeling with S46 (green) labeling the atrium, MF20 (blue) labeling the myocardium and Mef2 (red) labeling the cardiomyocyte nuclei in 48 hpf WT embryos (B, C) and *udu*−/− embryos without Tg(*hsp70l:nkx2.5-eGFP)* (B, D) and those harboring Tg(*hsp70l:nkx2.5-eGFP)* (C, E). Graphs showing the total number of cardiomyocytes (F), and a proportion of ventricular cardiomyocytes (G) in WT (grey) and *udu*$^{-/-}$ (blue) embryos with (light grey, light blue) and without Tg(*hsp70l:nkx2.5-eGFP)* (dark grey, dark blue). *p < 0.05, **p < 0.01, ***p < 0.001, ****p < 0.0001, error bars = SEM. Scale bar represents 50 μm.

nkx2.5 and *udu* genetically interact to maintain the correct proportion of ventricular cardiomyocytes.

4.6. Overexpression of nkx2.5 is not sufficient to suppress udu heart defects

We found that Gon4l regulates expression of *nkx2.5*, and that *nkx2.5* and *gon4l/udu* genetically interact to maintain the proportion of ventricular cardiomyocytes, raising the possibility that ventricular defects in *udu*$^{-/-}$ mutants result simply from reduced *nkx2.5* expression. To this end, we tested if overexpressing *nkx2.5* in *udu−/−* mutant embryos was sufficient to suppress ventricular fate deficiency. We generated *udu*$^{-/-}$; Tg(*hsp70l:nkx2.5-EGFP*)$^{+/-}$ embryos using the previously-validated Tg(*hsp70l:nkx2.5-EGFP*) transgenic line, which ubiquitously expresses *nkx2.5-EGFP* upon heat shock (George et al., 2015). Ectopic *nkx2.5* expression was induced via heat shock at 21-somite stage (Fig. 6 A), as evidenced by GFP expression that was visible within 1 h (data not shown) and which was then used to select embryos carrying the transgene (George et al., 2015). We analyzed cardiac chamber patterning and cardiomyocyte numbers using MF20, S46 and Mef2 IF in WT and *udu*$^{-/-}$ embryos with and without Tg(*hsp70l:nkx2.5*-eGFP) at 48 hpf (Fig. 6B–E). As a control, we first examined the effects of ectopic *nkx2.5* expression on WT cardiomyocytes. We found that heat-shocked WT embryos with the transgene exhibited no change in the total number of cardiomyocytes, or in the proportion of ventricular cells (205.0 ± 4.2, n = 6) relative to WT embryos without the transgene (207.3 ± 3.5, n = 7) (p = 0.68) (Fig. 6B and C, F, G). The total number of cardiomyocytes with ventricular identity was also unchanged in WT embryos with (101.3 ± 2.8, n = 6) and without the transgene (104.0 ± 2.6, n = 6).

Next, we tested the effects of the transgene activation in *udu* mutant embryos. We observed that the overall number of cardiomyocytes was unchanged in *udu*$^{-/-}$; Tg(*hsp70l:nkx2.5*-eGFP) (104.4 ± 6.7, n = 15) embryos compared to *udu*$^{-/-}$ mutant sibling control embryos (106.7 ± 4.4, n = 15) (p = 0.78) (Fig. 6 F). Likewise, *udu*$^{-/-}$ embryos carrying the Tg(*hsp70l:nkx2.5*-eGFP) (Fig. 6 E) did not exhibit a significant increase in the proportion of ventricular cardiomyocytes (43 ± 2.6, n = 15) relative to *udu−/−* siblings without the transgene that were subjected to heat shock (Fig. 6 D) (41 ± 1.6, n = 14) (p = 0.51) (Fig. 6 G). Consistent with these results, there was no change in the total number of cardiomyocytes with ventricular identity in *udu−/−* embryos with (42.2 ± 2.3, n = 15) or without the transgene (41.6 ± 3.4, n = 15). This result indicates that exogenous *nkx2.5* expression is not sufficient to normalize the number of cardiomyocytes (ventricular or otherwise) in *udu−/−* embryos. We interpret the inability of exogenous *nkx2.5-eGFP* expression to suppress the expansion of atrial identity in *udu−/−* embryos to indicate that Gon4l does not maintain ventricular identity solely through modulation of *nkx2.5* expression.

5. Discussion

Previous studies established a function for vertebrate Gon4l as a regulator of cell-cycle, apoptosis, somitogenesis, gastrulation movements, and blood development in zebrafish and mice (Barr et al., 2017; Hammerschimidt et al., 1996; Lim et al., 2009; Liu et al., 2007; Lu et al., 2010, 2011), but its involvement in heart development has not been previously examined. Here, we establish Gon4l as an essential regulator of cardiac development, including novel functions independent of its previously defined role in apoptosis. We found that in zebrafish embryos lacking zygotic *udu* function and exhibiting erythroid cell deficiencies (Liu et al., 2007), the initial formation and patterning of the heart tube was largely intact. During later stages of heart development, however, Gon4l is necessary for expansion of the cardiomyocyte pool by promoting their proliferation. Furthermore, *udu* genetically interacts with *nkx2.5* to maintain the proportion of ventricular cardiomyocytes, likely in part by promoting *nkx2.5* expression. Our studies, therefore, establish a novel role for the chromatin factor Udu/Gon4l in heart development (Fig. 7): Gon4l promotes cardiomyocyte proliferation and maintains the normal proportion of ventricular cardiomyocytes during zebrafish embryogenesis.

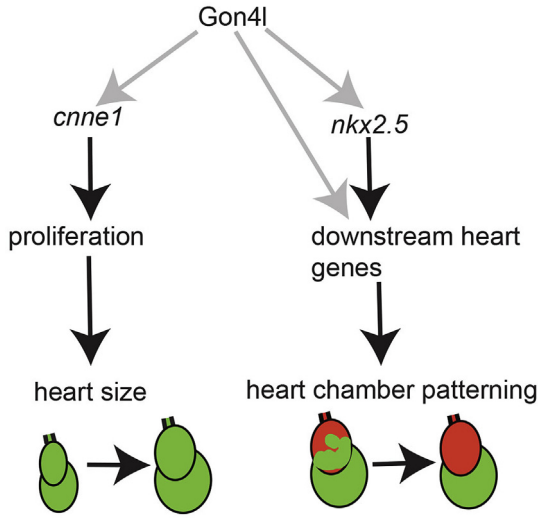

Fig. 7. Schematic depicting the roles of Gon4l in zebrafish heart development with the hypothesized functions in grey and the known roles in black.

This work highlights the role of Gon4l in cell cycle regulation during cardiomyocyte population expansion and is consistent with its previously described functions during zebrafish and mouse development in other tissues. However, key differences from preceding work emerge in our data. Our genetic interaction studies found that the reduction in cardiomyocyte numbers is TP53- and apoptosis independent (Fig. 2S), although we cannot rule out a contribution by TP53 or Casp3-independent mechanisms. This result contrasts with the *udu*$^{-/-}$ blood deficiency phenotype, which was partially suppressed by reduction of *tp53* expression using antisense morpholinos (Lim et al., 2009; Liu et al., 2007) and genetic maternal-zygotic loss of function (Fig. 2S). Our data, therefore, indicate that the cardiac defects arise through a distinct mechanism from the hematopoietic defects observed in the *udu*$^{-/-}$ mutants.

Additionally, we found that cardiomyocyte proliferation is reduced in *udu*$^{-/-}$ embryos, likely due to a failure to progress through S-phase of the cell cycle (Fig. 7). Gon4l has been linked to cell cycle regulation in both mouse and zebrafish (Barr et al., 2017; Lim et al., 2009), but there has been disagreement regarding which phase or phases of the cell cycle are disrupted upon loss of Gon4l function. In our study, we found that expression of *cnne2*, a gene necessary for the G1/S phase transition (Caldon, 2010), was down-regulated within the heart in *udu*$^{-/-}$ embryos at 36 hpf, while *cnnd3* exhibited increased expression (Fig. 3 H, J). DNA adenine methyltransferase identification (DamID-seq), a technique that detects protein-chromatin interactions (de Groote et al., 2012; Steensel, 2001), indicates that Gon4l is associated during gastrulation with the regulatory regions of *ccne2* and *cndd3*, as well other Cyclin genes, including *ccnd2a* and *ccnd2b*, suggesting Gon4l directly regulates expression of these genes (Fig. 3 F′, G′, H′, J′). One limitation of these DamID-Seq data is that they were obtained from whole embryos at late gastrula stage, and thus may not accurately reflect Gon4l association in a specific cell type and at later stages. Studies of multipotent blood progenitors in *Gon4l* mutant mouse found that *Ccnd* homologues are down-regulated during B-cell development while *Ccne* homologues were expressed at normal levels (Barr et al., 2017), indicating the role of Gon4l in regulating cell cycle genes is conserved, but the specific Cyclin-encoding genes regulated by this chromatin factor differ between species. In combination with previous studies, our results support an essential role for Gon4l in regulating G1/S check-point of the cell cycle (Barr et al., 2017; Lim et al., 2009). Furthermore, our findings that some *cyclin* genes exhibited increased levels of expression while the expression

levels of other *cyclin* genes was reduced support our previously published results that Gon4l can both positively and negatively regulate gene expression (Williams et al., 2018).

We also found that Gon4l is involved in the maintenance of the proportion of ventricular cardiomyocytes. Our findings open several possibilities regarding the relationship between *nkx2.5* and *udu/gon4l*. Our prior DamID-seq studies indicate that Gon4l is associated with the *nkx2.5* promoter during early zebrafish development (Fig. 4 M) (Williams et al., 2018). We further demonstrate that *udu* is necessary for the maintenance of *nkx2.5* expression during heart tube formation, and that *nkx2.5* genetically interacts with *udu* in regulating the proportion of ventricular cardiomyocytes (Fig. 5). However, exogenous expression of *nkx2.5* using the Tg(*hsp70l:nkx2.5*-eGFP) line did not restore the proper proportion of ventricular cardiomyocytes to *udu* mutants (Fig. 6B–G). This result indicates that Gon4l acts through *nkx2.5* and additional downstream factors, and/or in a parallel pathway, during maintenance of ventricular fate. Together, our results highlight the novel concept that epigenetic regulators play a role in preserving chamber-specific characteristics in the developing heart.

In conclusion, defining the precise roles of chromatin factors during cardiac development is an on-going process. This study elucidates previously unknown and essential roles for Gon4l during the processes of heart development after heart tube formation, adding to its previously recognized roles in convergence and extension gastrulation movements, somitogenesis and erythropoiesis (Liu et al., 2007; Lu et al., 2010; Siu et al., 2012; Williams et al., 2018). Based on these results we propose that Gon4l both promotes cell proliferation and regulates the expression of cardiac transcription factors to maintain the proportion of ventricular cardiomyocytes. The phenotypes we describe in *udu*$^{-/-}$ mutant embryos share similarities with the phenotypes for *hdac1*$^{-/-}$ mutant zebrafish embryos, namely in the reduced number of overall cardiomyocytes and specific reduction in ventricular cardiomyocytes (Song et al., 2019), bolstering support for potential interactions between Gon4l and Hdac1 in heart development. These findings describe a novel regulator of heart development and have the potential to provide insights into the mechanisms underlying congenital heart defects, ultimately facilitating directed therapeutic remediation in patients.

Acknowledgements

We thank Drs. Scott Higdon and Paul Gontarz for bioinformatics help. We thank Ms. Maggie Schedl, Ms. Gina Castelvecchi, and Mr. Ryan Beehler-Evans for technical assistance. The National Institutes of Health grants R01GM55101 and R35GM118179 to L.S.-K. RO1HL131438-02 to K.L.T. and F32GM113396 to M.L.K.W., and a W.M. Keck Foundation Fellowship to M.L.K.W. in part supported this study.

Appendix A. Supplementary data

Supplementary data to this article can be found online at https://doi.org/10.1016/j.ydbio.2020.03.002.

References

Alexander, J., Stainier, D.Y.R., Yelon, D., 1998. Screeening mosaic F1 females for mutations affecting zebrafish heart induction and patterning, 11. Developmental Genetics.

Bakkers, J., 2011. Zebrafish as a model to study cardiac development and human cardiac disease. Cardiovasc. Res. 91, 279–288.

Barr, J.Y., Goodfellow, R.X., Colgan, D.F., Colgan, J.D., 2017. Early B cell progenitors deficient for GON4L fail to differentiate due to a block in mitotic cell division. J. Immunol. 198, 3978–3988.

Bennett, J.S., Stroud, D.M., Becker, J.R., Roden, D.M., 2013. Proliferation of embryonic cardiomyocytes in zebrafish requires the sodium channel scn5Lab. Genesis 51, 562–574.

Berghmans, S., Murphey, R.D., Wienholds, E., Neuberg, D., Kutok, J.L., Fletcher, C.D., Morris, J.P., Liu, T.X., Schulte-Merker, S., Kanki, J.P., Plasterk, R., Zon, L.I., Look, A.T., 2005. tp53 mutant zebrafish develop malignant peripheral nerve sheath tumors. Proc. Natl. Acad. Sci. U. S. A. 102, 407–412.

Bodmer, R., 1993. The gene *tinman* is required for specification of the heart and visceral muscles in *Drosophila*. Development 118, 11.

Boyer, L., Latek, R., Peterson, C., 2004. The SANT domain: a unique histone-tail-binding module? Nat. Rev. 5, 6.

Buckingham, M., Meilhac, S., Zaffran, S., 2005. Building the mammalian heart from two sources of myocardial cells. Nat. Rev. Genet. 6, 826–835.

Burns, C.G., Milan, D.J., Grande, E.J., Rottbauer, W., MacRae, C.A., Fishman, M.C., 2005. High-throughput assay for small molecules that modulate zebrafish embryonic heart rate. Nat. Chem. Biol. 1, 263–264.

Cai, C., Liang, X., Shi, Y., Chu, P., Pfaff, S., Chen, J., Evans, S., 2003. Isl1 identifies a cardiac progenitor population that proliferates prior to differentiation and contributes a majority of cells to the heart. Development 5, 22.

Caldon, C., 2010. Distinct and redundant functions of cyclin E1 and cyclin E2 in development and cancer. Cell Div. 5.

Chen, J., Fishman, M.C., 1996. Zebrafish *tinman* homolog demarcates the heart field and initiates the myocardial differentiation. Development 122, 8.

de Groote, M.L., Verschure, P.J., Rots, M.G., 2012. Epigenetic Editing: targeted rewriting of epigenetic marks to modulate expression of selected target genes. Nucleic Acids Res. 40, 10596–10613.

De La Cruz, M.V., Gomez, C.S., Artega, M.M., Arguello, C., 1977. Experimental study of the development of the truncus and the conus in the chick embryo. J. Anat. 123, 25.

de Pater, E., Clijsters, L., Marques, S.R., Lin, Y.F., Garavito-Aguilar, Z.V., Yelon, D., Bakkers, J., 2009. Distinct phases of cardiomyocyte differentiation regulate growth of the zebrafish heart. Development 136, 1633–1641.

Deng, Z., Cao, P., Wan, M., Sui, G., 2010. Yin Yang 1 A multifaceted protein beyond a transcription factor. Transcription 1, 4.

Detrich, H.W., Kieran, M.W., Chan, F.Y., Barone, L.M., Yee, K., Rundstadler, J.A., Pratt, S., Ransom, D., Zon, L.I., 1995. Intraembryonic hematopietic cell migration during vertebrate development. Proc. Natl. Acad. Sci. Unit. States Am. 92, 5.

Dominguez, J.N., Meilhac, S.M., Bland, Y.S., Buckingham, M.E., Brown, N.A., 2012. Asymmetric fate of the posterior part of the second heart field results in unexpected left/right contributions to both poles of the heart. Circ. Res. 111, 1323–1335.

Dyer, L.A., Kirby, M.L., 2009. The role of secondary heart field in cardiac development. Dev. Biol. 336, 137–144.

Foglia, M.J., Poss, K.D., 2016. Building and re-building the heart by cardiomyocyte proliferation. Development 143, 729–740.

Galli, D., Dominguez, J.N., Zaffran, S., Munk, A., Brown, N.A., Buckingham, M.E., 2008. Atrial myocardium derives from the posterior region of the second heart field, which acquires left-right identity as Pitx2c is expressed. Development 135, 1157–1167.

Gansner, J.M., Madsen, E.C., Mecham, R.P., Gitlin, J.D., 2008. Essential role for fibrillin-2 in zebrafish notochord and vascular morphogenesis. Dev. Dynam. 237, 2844–2861.

George, V., Colombo, S., Targoff, K.L., 2015. An early requirement for nkx2.5 ensures the first and second heart field ventricular identity and cardiac function into adulthood. Dev. Biol. 400, 10–22.

Gregoire, S., Karra, R., Passer, D., Deutsch, M.A., Krane, M., Feistritzer, R., Sturzu, A., Domian, I., Saga, Y., Wu, S.M., 2013. Essential and unexpected role of Yin Yang 1 to promote mesodermal cardiac differentiation. Circ. Res. 112, 900–910.

Hammerschimidt, M., Pelegri, F., Mullins, M., Kane, D., Brand, M., van Eeden, J., Furtani-Selki, M., Granato, M., Haffter, P., Heisenberg, C.P., Jiang, Y.J., Kelsh, R., Odenthal, J., Warga, R., Nusslein-Volhard, C., 1996. Mutations affecting morpohgenesis during gastrulation and tail formation in the zebrafish, *Danio rerio*. Development 123, 9.

Harvey, R.P., Lai, D., Elliot, D., Biben, C., Solloway, M., Prall, O., Stennard, R., Schindeler, A., Groves, N., Lavulo, L., Hyun, C., Yeoh, T., Costa, M., Furtado, M., Kirk, E., 2002. Homeodomain factor Nkx2.5 in heart development and disease. Cold Spring Harbor Symp. Quant. Biol. 67, 107–114.

Huang, C.J., Tu, C.T., Hsiao, C.D., Hsieh, F.J., Tsai, H.J., 2003. Germ-line transmission of a myocardium-specific GFP transgene reveals critical regulatory elements in the cardiac myosin light chain 2 promoter of zebrafish. Dev. Dynam. 228, 30–40.

Jay, P.Y., Berul, C.I., Tanaka, M., Ishii, M., Kurachi, Y., Izumo, S., 2003. Cardiac conduction and arrhythmia: insight from Nkx2.5 mutations in mouse and humans. Novartis Found. Symp. 250, 227–238.

Jung, J., Kim, T.G., Lyons, G.E., Kim, H.R., Lee, Y., 2005. Jumonji regulates cardiomyocyte proliferation via interaction with retinoblastoma protein. J. Biol. Chem. 280, 30916–30923.

Just, S.R.L., Berger, I., Buhler, A., Kebler, M., Rottbauer, W., 2016. Tbx20 Is an Essential Regulator of Embryonic Heart Growth in Zebrafish. PloS One.

Kimelman, D., 2006. Mesoderm induction: from caps to chips. Nat. Rev. Genet. 7, 360–372.

Kimmel, C., Ballard, W., Kimmel, S., Ullman, B., Schilling, T., 1995. Stages of embryonic development of the zebrafish. Dev. Dynam. 203, 17.

Kook, H., Lepore, J.J., Gitler, A.D., Lu, M.M., Wing-Man Yung, W., Mackay, J., Zhou, R., Ferrari, V., Gruber, P., Epstein, J.A., 2003. Cardiac hypertrophy and histone deacetylase–dependent transcriptional repression mediated by the atypical homeodomain protein Hop. J. Clin. Invest. 112, 863–871.

Lee, K.H., Xu, Q., Breitbart, R.E., 1996. A New tinman-Related Gene, nkx2.7, Anticipates the Expression of nkx2.5 and nkx2.3. In: Zebrafish Heart and Pharyngeal Endoderm Developmental Biology, vol. 180, p. 9.

Leone, M., Magadum, A., Engel, F.B., 2015. Cardiomyocyte proliferation in cardiac development and regeneration: a guide to methodologies and interpretations. Am. J. Physiol. Heart Circ. Physiol. 309, H1237–H1250.

Lickert, H., Tekeuchi, J., von Both, I., Walls, J., McAuliffe, J., Rossant, J., Brueneau, B., 2004. Baf60c is essential for function of BAF chromatin remodeling complexes in heart development. Nature 432.

Lickert, Takeuchi, J.V.B.I., Walls, J.R., McAuliffe, F., Adamson, S.L., Henkelman, R.M., Wrana, J.L., Rossant, J., Bruneau, B.G., 2004. Baf60c is essential for function of BAF

chromatin remodelling complexes in heart development. Nature 432 (7013), 107–112.
Lim, C., Chong, S., Jiang, Y.J., 2009. Udu deficiency activates DNA damage checkpoint. Mol. Biol. Cell 20, 11.
Liu, Y., Du, L., Osato, M., Teo, E.H., Qian, F., Jin, H., Zhen, F., Xu, J., Guo, L., Huang, H., Chen, J., Geisler, R., Jiang, Y.J., Peng, J., Wen, Z., 2007. The zebrafish udu gene encodes a novel nuclear factor and is essential for primitive erythroid cell development. Blood 110, 99–106.
Lombardo, V.A., Otten, C., Abdelilah-Seyfried, S., 2015. Large-scale zebrafish embryonic heart dissection for transcriptional analysis. J Vis Exp 95, 52087.
Lu, P., Hankel, I.L., Hostager, B.S., Swartzendruber, J.A., Friedman, A.D., Brenton, J.L., Rothman, P.B., Colgan, J.D., 2011. The developmental regulator protein Gon4l associates with protein YY1, co-repressor Sin3a, and histone deacetylase 1 and mediates transcriptional repression. J. Biol. Chem. 286, 18311–18319.
Lu, P., Hankel, I.L., Knisz, J., Marquardt, A., Chiang, M.Y., Grosse, J., Constien, R., Meyer, T., Schroeder, A., Zeitlmann, L., Al-Alem, U., Friedman, A.D., Elliott, E.I., Meyerholz, D.K., Waldschmidt, T.J., Rothman, P.B., Colgan, J.D., 2010. The Justy mutation identifies Gon4-like as a gene that is essential for B lymphopoiesis. J. Exp. Med. 207, 1359–1367.
Matrone, G., Tucker, C.S., Denvir, M.A., 2017. Cardiomyocyte proliferation in zebrafish and mammals: lessons for human disease. Cell. Mol. Life Sci. 74, 1367–1378.
Montgomery, R.L., Davis, C.A., Potthoff, M.J., Haberland, M., Fielitz, J., Qi, X., Hill, J.A., Richardson, J.A., Olson, E.N., 2007. Histone deacetylases 1 and 2 redundantly regulate cardiac morphogenesis, growth, and contractility. Genes Dev. 21, 1790–1802.
Nakajima, K., Inagawa, M., Uchida, C., Okada, K., Tane, S., Kojima, M., Kubota, M., Noda, M., Ogawa, S., Shirato, H., Sato, M., Suzuki-Migishima, R., Hino, T., Satoh, Y., Kitagawa, M., Takeuchi, T., 2011. Coordinated regulation of differentiation and proliferation of embryonic cardiomyocytes by a jumonji (Jarid2)-cyclin D1 pathway. Development 138, 1771–1782.
Nambiar, R.M., Ignatius, M.S., Henion, P.D., 2007. Zebrafish colgate/hdac1 functions in the non-canonical Wnt pathway during axial extension and in Wnt-independent branchiomotor neuron migration. Mech. Dev. 124, 682–698.
Nan, C., Huang, X., 2009. Transcription factor Yin Yang 1 represses fetal troponin I gene expression in neonatal myocardial cells. Biochem. Biophys. Res. Commun. 378, 62–67.
Ohtani, K., Zhao, C., Dobreva, G., Manavski, Y., Kluge, B., Braun, T., Rieger, M.A., Zeiher, A.M., Dimmeler, S., 2013. Jmjd3 controls mesodermal and cardiovascular differentiation of embryonic stem cells. Circ. Res. 113, 856–862.
Paige, S.L., Plonowska, K., Xu, A., Wu, S.M., 2015. Molecular regulation of cardiomyocyte differentiation. Circ. Res. 116, 341–353.
Pierpont, M.E., Basson, C.T., Benson Jr., D.W., Gelb, B.D., Giglia, T.M., Goldmuntz, E., McGee, G., Sable, C.A., Srivastava, D., Webb, C.L., American Heart Association Congenital Cardiac Defects Committee, C.o.C.D.i.t.Y, 2007. Genetic basis for congenital heart defects: current knowledge: a scientific statement from the American heart association congenital cardiac defects committee, council on cardiovascular disease in the young: endorsed by the American academy of pediatrics. Circulation 115, 3015–3038.
Pradhan, A., Zeng, X.I., Sidhwani, P., Marques, S.R., George, V., Targoff, K.L., Chi, N.C., Yelon, D., 2017. FGF signaling enforces cardiac chamber identity in the developing ventricle. Development 144, 1328–1338.
Rana, M.S., Theveniau-Ruissy, M., De Bono, C., Mesbah, K., Francou, A., Rammah, M., Dominguez, J.N., Roux, M., Laforest, B., Anderson, R.H., Mohun, T., Zaffran, S., Christoffels, V.M., Kelly, R.G., 2014. Tbx1 coordinates addition of posterior second heart field progenitor cells to the arterial and venous poles of the heart. Circ. Res. 115, 790–799.
Reifers, F., Walsh, E., Leger, S., Stainier, D.Y., Brand, M., 2000. Induction and differentiation of the zebrafish heart requires fibroblast gorwth factor 8 (*fgf8/acerebellar)*. Development 127, 11.
Rohr, S., Bit-Avragim, N., Abdelilah-Seyfried, S., 2006. Heart and soul/PRKCi and nagie oko/Mpp5 regulate myocardial coherence and remodeling during cardiac morphogenesis. Development 133, 107–115.
Salic, A., Mitchison, T.J., 2008. A chemical method for fast and sensitive detection of DNA synthesis in vivo. Proc. Natl. Acad. Sci. U. S. A. 105, 2415–2420.
Sankaran, V.G., Ludwig, L.S., Sicinska, E., Xu, J., Bauer, D.E., Eng, J.C., Patterson, H.C., Metcalf, R.A., Natkunam, Y., Orkin, S.H., Sicinski, P., Lander, E.S., Lodish, H.F., 2012. Cyclin D3 coordinates the cell cycle during differentiation to regulate erythrocyte size and number. Genes Dev. 26, 2075–2087.
Siu, K.T., Rosner, M.R., Minella, A.C., 2012. An integrated view of cyclin E function and regulation. Cell Cycle 11, 57–64.
Song, Y.C., Dohn, T.E., Rydeen, A.B., Nechiporul, A.V., Waxman, J.F., 2019. HDAC1-mediated repression of the retinoic acid-responsive gene *ripply3* promotes second heart field development. PLoS Genet. 15 (5), e1008165.
Stainier, D.Y., 2001. Zebrafish genetics and vertebrate heart formation. Nat. Rev. 2.
Steensel, B., Delrow, J., Henikoff, S., 2001. Chromatin profiling using targeted DNA adenine methyltransferase. Nat. Genet. 27, 5.
Takeuchi, J.K., Lou, X., Alexander, J.M., Sugizaki, H., Delgado-Olguin, P., Holloway, A.K., Mori, A.D., Wylie, J.N., Munson, C., Zhu, Y., Zhou, Y.Q., Yeh, R.F., Henkelman, R.M., Harvey, R.P., Metzger, D., Chambon, P., Stainier, D.Y., Pollard, K.S., Scott, I.C., Bruneau, B.G., 2011. Chromatin remodelling complex dosage modulates transcription factor function in heart development. Nat. Commun. 2, 187.
Targoff, K.L., Colombo, S., George, V., Schell, T., Kim, S.H., Solnica-Krezel, L., Yelon, D., 2013. Nkx genes are essential for maintenance of ventricular identity. Development 140, 4203–4213.
Targoff, K.L., Schell, T., Yelon, D., 2008. Nkx genes regulate heart tube extension and exert differential effects on ventricular and atrial cell number. Dev. Biol. 322, 314–321.
Thisse, C., Thisse, B., 2008. High-resolution in situ hybridization to whole-mount zebrafish embryos. Nat. Protoc. 3, 59–69.
Ticho, B., Stainier, D., Fishman, M.C., Breitbart, R.E., 1996. Three zebrafish MEF2 genes delineate somitic and cardiac muscle development in wild-type and mutant embryos. Mech. Dev. 59, 13.
Triedman, J.K., Newburger, J.W., 2016. Trends in congenital heart disease: the next decade. Circulation 133, 2716–2733.
Tu, C.T., Yang, T.C., Tsai, H.J., 2009. Nkx2.7 and Nkx2.5 function redundantly and are required for cardiac morphogenesis of zebrafish embryos. PloS One 4, e4249.
Van Vliet, P., Wu, S.M., Zaffran, S., Puceat, M., 2012. Early cardiac development: a view from stem cells to embryos. Cardiovasc. Res. 96, 352–362.
Vincent, S.D., Buckingham, M.E., 2010. How to Make a Heart 90, 1–41.
Williams, M.L.K., Sawada, A., Budine, T., Yin, C., Gontarz, P., Solnica-Krezel, L., 2018. Gon4l regulates notochord boundary formation and cell polarity underlying axis extension by repressing adhesion genes. Nat. Commun. 9 (1), 1319.
Yang, J., Xu, X., 2012. Immunostaining of dissected zebrafish embryonic heart. J Vis Exp, e3510.
Yelon, D., Horne, S., Stainier, D.Y., 1999. Restricted expression of cardiac myosin genes reveals regulated aspects of heart tube Assembly in zebrafish. Dev. Biol. 214, 15.
Yelon, D., Ticho, B., Halpern, M., Ruvinsky, I., Ho, R., Silver, L., Stainier, D., 2000. The bHLH transcription factor hand2 plays parallel roles in zebrafish heart and pectoral fin development. Development 127.
Yelon, D.H.S.D.S., 1999. Restricted expression of cardiac myosin genes reveals regulated aspects of heart tube Assembly in zebrafish. Dev. Biol. 214, 15.
Yutzey, K., Gannon, M., Bader, D., 1995. Diversification of cardiomyogenic cell lineages in vitro. Dev. Biol. 10.
Yutzey, K., Rhee, J., Bader, D., 1994. Expression of the atrial-specific myosin heavy chain AMHC1 and the establishment of anteroposterior polarity in the developing chicken heart. Development 12.
Zaffran, S., 2002. Early signals in cardiac development. Circ. Res. 91, 457–469.
Zaffran, S., Kelly, R.G., Meilhac, S.M., Buckingham, M.E., Brown, N.A., 2004. Right ventricular myocardium derives from the anterior heart field. Circ. Res. 95, 261–268.